MetaMesh: a Hierarchical Computational Model for Design and Fabrication of Biomimetic Armor Surfaces

Jorge Duro-Royo[1]*, Katia Zolotovsky[2]*, Laia Mogas-Soldevila[1], Swati Varshney[3], Neri Oxman[1], Mary C. Boyce[4], and Christine Ortiz[3]

[1] *MIT Media Lab*
[2] *Department of Architecture*
[3] *Department of Materials Science and Engineering*
[4] *Department of Mechanical Engineering*
 Massachusetts Institute of Technology, 77 Massachusetts Avenue, Cambridge MA 02139
*These authors contributed equally to this work*

KEYWORDS

Biomimetics, bio-inspired design, computational design, hierarchical computation, adaptation, mesh data structure, multi-functional, natural exoskeletons

HIGHLIGHTS

- *MetaMesh* is a hierarchical computational construct to generate articulated armored surfaces
- The ancient armored fish *Polypterus senegalus* provides source of bio-inspiration
- Local, regional and global levels of organization embed functional differentiation
- Articulation of scale units is preserved by neighborhood morphing techniques
- The model is adaptable to a wide array of complex hosting surfaces

GRAPHICAL ABSTRACT
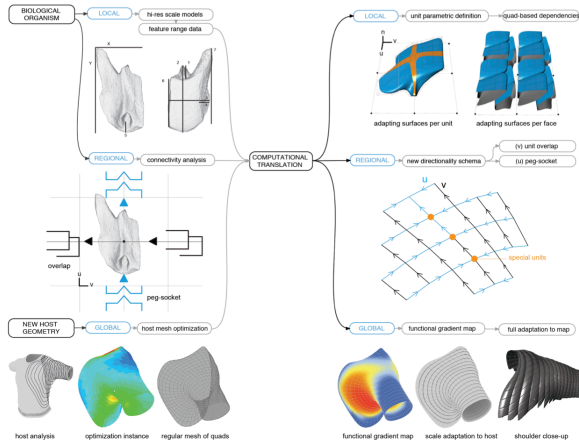
ABSTRACT

Many exoskeletons exhibit multifunctional performance by combining protection from rigid ceramic components with flexibility through articulated interfaces. Structure-to-function relationships of these natural bioarmors have been studied extensively, and initial development of structural (load-bearing) bioinspired armor materials, most often nacre-mimetic laminated composites, has been conducted. However, the translation of segmented and articulated armor to bioinspired surfaces and applications requires new computational constructs. We propose a novel hierarchical computational model, *MetaMesh,* that adapts a segmented fish scale armor system to fit complex "host surfaces." We define a "host" surface as the overall geometrical form on top of which the scale units are computed. *MetaMesh* operates in three levels of resolution: (i) *locally* - to construct unit geometries based on shape parameters of scales as identified and characterized in the *Polypterus senegalus* exoskeleton, (ii) *regionally* - to encode articulated connection guides that adapt units with their neighbors according to directional schema in the mesh, and (iii) *globally* - to generatively extend the unit assembly over arbitrarily curved surfaces through global mesh optimization using a functional coefficient gradient. Simulation results provide the basis for further physiological and kinetic development. This study provides a methodology for the generation of biomimetic protective surfaces using segmented, articulated components that maintain mobility alongside full body coverage.

1. INTRODUCTION

Structural materials in nature achieve diverse functions such as toughness, flexibility and strength, through spatial variation in material properties and morphometry across organizational hierarchies with precise interfacial control [1-2]. Biologically inspired engineering, or the translation of design schema in nature, being chemical, physical, genetic, or geometric, to synthetic systems requires complex models that both capture the intricacies of biological models and adapt their multi-scale design principles to new operative constraints. The process of mapping functional requirements between design solutions presents several theoretical and technical challenges to ensure continuity and coherence of all components. With the advent of high resolution materials characterization methods, powerful computational simulation capabilities, and increasingly precise digital fabrication technologies, it is now becoming possible to develop novel multifunctional structures with intricate, interactive, and hierarchical design strategies inspired by biological models.

The study of biological armor systems is an emerging field [3-7] with recent initial development of structural (load-bearing) bioinspired armor materials, most often nacre-mimetic [8]. However, the design and manufacture of a bioinspired exoskeleton including salient local-regional-global hierarchical features have yet to be realized. In this paper, we present a computational design methodology that combines scientific analytical methods and computational form finding tools to generate a flexible protective surface based on an armored fish exoskeleton. Our biological model is the exoskeleton of the ancient fish, Polypterus senegalus. Its armor **(Figure 1a)** is composed of articulated, mineralized scales that act as a protective medium from predatory threats while also allowing biomechanical flexibility in axial bending and torsion [3, 9-13]. The functional framework of the fish scale jacket **(Figure 1b)** uses spatial variation of unit morphometry (size and shape) and their arrangement into semi-helical rings to balance the two seemingly contradictory functions of full coverage and mobility. Our prior research has begun to explore the geometric design rules underpinning the functional framework [14-16]. One of our previous models constructed a parametric definition of single scale geometries and an associative model to generate an array of homogeneous scales using computer-aided design (CAD) software for multi-material 3D printing of a flexible, flat surface [14]. Another model morphed scale-based geometries along a sequence to determine dimensional parameters that can be varied while maintaining connectivity within a single direction [15].

Our goal is to create a generative computational design framework for functionally graded structures with tunable local performance. These local performances can adapt to any given hosting mesh surface by emulating the design principles observed in the flexible fish exoskeleton. We distill the geometric design rules underlying the *P. senegalus* exoskeleton across multiple length scales (local, regional, and global). We then present the *MetaMesh* model that translates these design rules hierarchically to a synthetic system using an efficient framework linking experimental analytical methods (X-ray micro-computed tomography and morphometric analysis) with advanced computational geometry techniques (custom data structures for polygon mesh processing and component adaptation). *MetaMesh* operates in three levels of resolution: (i) locally - to construct unit geometries based on shape parameters of scales in the *P. senegalus* exoskeleton, (ii) regionally - to encode articulated connection guides that adapt units with their neighbors according to directional schema in the mesh, and (iii) globally - to generatively extend the unit assembly over arbitrarily curved surfaces through global mesh optimization using a functional coefficient gradient. Unlike component-based parametric techniques that focus on the packed placement of self-similar units over surfaces [17], *MetaMesh* incorporates complex connectivity and overlap of the units to enable articulation with neighbors. In addition, through functional variation in unit shape, it allows control over regional connectivity and interlocking between units. We demonstrate the *MetaMesh* model's potential with its application to a human body mesh surface and further discuss the model's advantages and limitations. This computational adaptation of an articulated, segmented, flexible surface serves as a proof-of-concept model for enhanced biomimetic structures in various fields such as transportation (e.g. ground, air, water, or space), architecture (e.g. building skins or canopies), sports and military (e.g. personal protection), and consumer products (e.g. packaging) [12, 14].

2. MATERIALS AND METHODS

2.1 X-ray Micro-computed Tomography (µCT)

Eleven scales were excised from a deceased *P. senegalus* specimen (every 10th scale across a row on the left side of the body) and scanned via x-ray micro-computed tomography (µCT; Viva CT40, Scanco Medical AG,

Switzerland) operated at 45kV and 177μA. The microtomographic data was reconstructed using bilinear and inter-plane interpolation algorithms into polygonal meshes using an interactive medical imaging software (MIMICS® 14.1, Materialise, Belgium) to generate digital 3D objects of the scales in sterolithography (STL) format. Further processing was executed in Rhino3D (RHINOCEROS®, Robert McNeel and Associates, USA) to remove noise and internal porosity.

2.2 Morphometric Analysis

Geometric analysis measured variation in scale shape and served as a basis for the computational model. The coordinates of twenty landmarks defining the outline of the scale including all geometrical features were extracted from the 3D STL objects using a custom Visual Basic code programmed in the Rhino3D environment. These landmark coordinates were subjected to translation, rotation, and scaling relative to the centroid. Magnitudes of relative geometric parameters were calculated based on the coordinates. The volume of the scale was measured from the STL file in Rhino3D.

2.3 Computational Modeling

The computational framework defining the *MetaMesh* data structure (local scale geometric definition, regional directionality patterns, and global functional gradient application) was implemented in C# on top of the design platform in Rhino3D. The mesh optimization process was implemented in Java (Eclipse IDE, © 2013 The Eclipse Foundation) and deployed within a customized applet.

2.4 Multi-material 3D Printing

The closed-surface multi-material prototypes were designed using parametric CAD software (SOLIDWORKS®, Dassault Systèmes SolidWorks Corp., France) as described by Reichert et al. for a flat surface [14]. The components of the prototype were exported as separate STL files per material component and fabricated using multi-material 3D printing (using digital materials from OBJET Connex500™) with 30 μm resolution in the digital mode. Rigid components were printed with VeroWhite (Objet FullCure® 830) and compliant components were printed with TangoPlus (Objet FullCure® 930).

3. RESULTS

3.1 Biological Exoskeleton Design Rules

The geometric design rules in the *P. senegalus* exoskeleton are characterized across three levels of resolution: local, regional, and global. The individual scales have varying geometries, are articulated with each other to allow flexibility alongside full body coverage, and are organized in a long-range surface over the entire fish body. These design components are formed during the organism's growth and are thus inseparable; however, we distinguish amongst these levels of resolution for ease of translation using the computational model.

3.1.1 Local

The local level of organization relates to a single scale, its anatomy, and its geometric variation. The scales of the organism are highly mineralized and display a multilayered internal composite structure with a consistent material composition throughout the exoskeleton [3,12,13]. The geometrical features of the scales (**Figure 2a**, left) include: a protruding peg (P) and a corresponding socket (S) that articulates neighboring scales within a single column of scales (paraserially) and constrains relative motion; the anterior process (AP), a large extension that overlaps with the scales in the next column (interserially) and enables scales to slide relative to each other; and the axial ridge (AR), a protrusion on the underside of the scale that connects the scale to the underlying skin. Based on line lengths and angles between features on the scale (**Figure 2a**, left), eight parameters were calculated for morphometric analysis of the fish scales (**Figure 2a**, right): relative length peg to scale (PSL), shape aspect ratio as the length of peg-and-socket axis divided by scale width (SR), bounding box size (E), interserial overlap with the adjacent scale in the next column along v-axis (IO), paraserial overlap with the adjacent scale in the same column along u-axis (PO), relative edge degrees (ANG), anterior process length (APL), and volume (VOL).

The scale geometry varies gradually relative to its position in the exoskeleton [9], as illustrated in the digitally-reconstructed μCT images of subset of 11 *P. senegalus* scales lying in the same row from head to tail (labeled by their column position in the exoskeleton, C1-50) in **Figure 2b**. Values for the eight shape parameters for these scales are tabulated and plotted as normalized quantities in **Figure 2b**. The scales exhibit a general trend of feature reduction from head to tail. For instance, in the tail region, variants C45-C50 have smaller magnitudes of the two articulating joints (PSL, IO) compared to front region variants C1-10. The PSL diminishes gradually from 0.22 to 0.03 in scales from head to tail. In the front region, the peg-and-socket joint plays a functional role in stiffening the column of scales, while in the tail region, the lack of peg-and-socket allows scales within a column to move freely relative to each other. The IO between columns also decreases from 0.28 to 0.13, thus compromising the relative sliding between columns. These parameters further relate to regional connectivity between columns as discussed in the next sections.

3.1.2 Regional

The regional level of organization describes the interconnectivity of fish scales in the exoskeleton and the correlation between local shape variation and regional functionality of the system. Two articulating joint structures define the standard unit schema between a single scale and its neighbors as shown in schematic views in **Figure 3a**: the peg-and-socket joint connects scales down a column (paraserially) while the overlap joint allows interscale sliding between columns (interserially). The geometry of these joints further defines the rotational degrees of freedom, e.g. bending and twisting, that scales have in moving relative to each other (**Figure 3b**). The overlap joint allows bending, sliding, and twisting, while peg and socket joint allows only limited bending and rotation around its axis [9]. In the construction of the computational model in Section 3.2, we define the axis of peg-and-socket joints as the *u-direction (paraserial)* and the axis of the overlap joint as v-*direction (interserial);* these are two consistently identifiable directions between any set of adjacent scales.

Two fibrous, organic components hold the scales together in the armor: the *stratum compactum* and *Sharpey's fibers*, illustrated in **Figure 3c**. The *stratum compactum* is a crisscrossed, layered tissue composed of collagenous fibers that attach the scales to the underlying skin [9]. The fibers are aligned along the paraserial and interserial directions in alternating layers. The *Sharpey's fibers* are short fibers that connect the peg and socket of adjacent scales [9]. These fibers support and align the peg and socket joint, and allow the paraserial column of scales to withstand compressive and tensile stresses.

The degrees of freedom in relative motion are dependent on the geometric parameters of the scales. **Figure 4** demonstrates the difference in ranges of motion between two shape variants: a head region scale and a tail region scale. The head region scale (**Figure 4a-d**) is bigger and possesses more pronounced shape features: the well-pronounced peg and socket as well as the paraserial overlap restrict rotation between scales within a single column, while the large anterior process enables relative sliding resulting in significant changes in overlap between scales (42-110% [9]) as the exoskeleton bends to extreme curvatures. This variant shows full contact between the scales with additional overlap in peg-and-socket direction and requires additional bending **(Figure 4a)** or translation **(Figure 4b)** to rotate around the peg axis. In contrast, in the tail region scale (**Figure 4e-h**), the anterior process is smaller and has a simpler rhomboid shape, which relaxes the paraserial constraints while still allowing interserial sliding to accommodate the rapid undulation of the tail in steady-state swimming.

3.1.3 Global

The global level of organization relates the long-range assembly of the scales across the body of the fish to its kinetic motion. Semi-helical columns of 'standard unit' scales are aligned with their peg and socket joint running top to bottom, and overlap running from head to tail (**Figure 5a**). These columns of scales are symmetric on the right and left sides of the fish body, and are connected by top and bottom midlines composed of units with a specialized geometry. Two types of specialized units exist in the fish; double-peg unit on the top line and double socket on the bottom line (**Figure 5b**). Lines of symmetry on the top and bottom of fish trunk possess specialized units (orange) with double pegs and double sockets that receive columns on both sides (blue). The scale shapes and joint configurations are tailored to the varying radius of curvature throughout the structural ring (**Figure 5c-e**).

The orientation of scales within the assembly exoskeleton further contributes to functional variation within the armor. The structural rings and underlying fibrous tissue have an oblique orientation to the main axis of the trunk, which ranges from 60° in the front region to 45° in the back region [9] as shown in **Figure 6a.** The front 60° orientation is optimal for extreme curvatures in helical arrangement, as found in eels and worms [18], while the rigid peg-and-socket joint sustains the helical component of the torsional strain [9]. The back region 45° orientation is optimal for restricting torsion in steady-state swimming [19]. Furthermore, the angle between the edges of the scale (ANG) also decreases gradually from 87°-60°, from head to tail, showing that the directionality of the paraserial and interserial axes are regionally adapted to the global kinetic motion of the fish. Local scale geometry further contributes to the functional variation of the armor. A functional coefficient (FC) was calculated as the average value of the normalized geometric parameters PSL, IO, PI, and AP. The FC is mapped onto the fish exoskeleton in **Figure 6a**. The FC indicates how developed the connective interfaces are between adjacent scales, i.e. how constrained the peg and socket joint is along the paraserial direction compared with overlap sliding along the interserial direction, ranging from 0 (maximum protection) to 1 (maximum flexibility). As a consequence of the local scale geometry and regional orientation, the long range assembly of scales is capable of achieving high radii of curvature throughout the exoskeleton, e.g. in the fast-start escape response depicted in **Figure 6b**.

3.2 MetaMesh: Hierarchical Computational Model

Our hierarchical computational model, *MetaMesh*, unpacks the organism-specific design principles and applies them, in a generative way, to a different host surface with new functional specifications. *MetaMesh* creates and maintains consistent neighborhood relationships for the three-dimensional articulated surfaces of units on a quadrilateral polygonal mesh. The mesh data structure tailored for this model is designed to meet specific topological, algorithmic, and data access requirements.

The topology of our structure is a high-resolution polygonal regular mesh of quads with boundaries. The three components of a polygon mesh (vertices, edges, or faces) determine the connectivity between the mesh elements [20]. To ensure smooth connectivity between component features, each vertex holds one scale unit and each face shares the information of four scale geometries**.** We specify meshes with boundaries, defined by edges incident to only one face [21] to include neckline and sleeve openings. The paraserial and interserial axes in the fish exoskeleton are translated onto the u- and v- directions of the parametric surface subdivision**.**

Algorithmic requirements operate on unit orientation and connectivity along u- and v- directions, as well as on unit geometry adaptation to new vertex positions through mesh optimization. Furthermore, our model takes into account functional gradients of protection and flexibility mapped on the human body. In order to preserve smooth continuity of the functional changes over the host surface, the model associates extra geometry to the vertices, edges, and faces of the mesh to share geometrical data with neighboring elements. To do this, we used a finite set of vertex indices (V), a table of 3D vertex coordinates $X = \{x_i: I \in V\}$, and a set of polygon faces (F), in which a face $f = (i_1 \ldots i_{nf})$ is a sequence of non-repeating vertex indices [22].

We further impose access requirements to the sets of data included in the model. The data sets for vertices, edges, and faces are accessible by enumeration of all elements and the oriented transversal of face edges. Given an edge, we are able to access its starting and end vertices. Given a vertex, at least one attached face or edge must be accessible while all other elements in the neighborhood of the vertex (i.e. incident faces, edges, or neighboring vertices) can be enumerated [23].

Our hierarchical computational model, *MetaMesh*, is designed to meet these requirements at three organizational levels following the geometric rules of assembly: (i) local definition of a standard unit and construction of different unit geometries in association with their neighbors, (ii) regional application of directional patterns and functional gradients that define the locations of different units, and (iii) global optimization of the host mesh to reposition vertices that affect local adaptation of unit shapes.

3.2.1 Local

The local level of organization captures the standard scale unit (S) as a building block by taking into account the features of its neighbors and the underlying host mesh geometry (**Figure 7**). Each scale unit is centered on top of one mesh vertex and constructed through a set of controllable parameters (**Figure 7a**). Since each vertex has an associated unit, its geometry can adapt to the host surface curvature. The local set of information per mesh face contains shared data between four units, which takes into account the features of neighboring scales. Each vertex stores the information of four parameters that will affect its associated unit schema in two different directions. Along the u-direction (paraserial), the unit geometry is influenced by the PSL, PO, and APL parameters. Along the v- direction (interserial), the unit geometry and lateral scale superposition are influenced by IO.

Specific parametric dimensions are calculated to determine unit features and their position on the quad in order to unite the underlying mesh with the geometrical parameters and functional requirements of the host surface, described further in Section 3.3.2. A particular vertex is defined as $V_0(i,j)$, and its four neighbor vertices are defined as $V_1(u+1,v)$, $V_2(u-1,v)$, $V_3(u,v+1)$, $V_4(u,v-1)$ as shown in **Figure 7a**. The midpoints of their edges are then defined as m_{4-0}, m_{0-1}, m_{0-3}, m_{2-0}. **Figure 7b** shows how the unit is constructed from four connecting surfaces for each adjacent mesh quad (blue) and resulting cross-shaped contact surface centered in the vertex (orange). The unit lengths are calculated as shown in the table below and then mapped onto the mesh quads using a unit square bilinear interpolation algorithm [24], as shown in **Figure 7c,** where an unknown function f at point $X(u,v)$ is found with respect to a unit quad of points $P_1(1,0)$, $P_2(1,1)$, $P_3(1,0)$ and $P_4(0,0)$. We perform a linear interpolation between P_1 and P_2 resulting in point $A(u,v)$ and another linear interpolation between point P_3 and P_4 resulting in point $B(u,v)$ providing an estimate for $f(u,v)$: $f{u,v} = f{0,0}1-u1-v + f{1,0}u1-v + f{1-uv} + f{1,1}uv$

Scale Width	L8	$= m_{4-0} - m_{0-3}$
AP Length	L6	$= m_{2-0} - m_{0-1}$
PO Length	L7	$= APL / L6.$
Overall Length	L2	$= L1 + L5 + L6$, where $L1 = L2 * PSL$ and $L5 = L2 * PO$
		$= L6 / (1-(PSL+PO))$
Overall Width	L3	$= L8 + L4$, where $L4 = L3 * IO$,
		$= L8 / (1-IO)$

The u- and v- directions act as guides for the construction of the peg-socket and overlap connections in a unit. In MetaMesh computation each side of a quad can host either u- or v- direction and this allows definition of new types of specialized units in addition to the ones found in the fish (e.g. A, B, C in **Figure 7d**). The double-peg and double-socket units in the top and bottom midlines in the fish (e.g. D, E in **Figure 7d**) are defined as variations from the standard scale through the encoded u- and v- directions**.** This method of specialized units enabling polygonal mesh connectivity is similar to the stitch mesh method developed by Yuksel et al. for yarn patterns in 2.5D, where course and wale edges have an extra layer of information to define the connectivity of the yarn elements at the mesh edges [25].

3.2.2 Regional

The regional level of organization orients mesh regions against the hosting surface. A mesh is defined as "orientable" if all faces (i.e. normal vectors for all polygons) point consistently to the same side of the mesh. The information encoded in our u- and v- directions does not affect the orientability of the mesh, but tailors edge directionality as extra regional data in the data structure. **Figure 8** illustrates the directionality analysis of a human shoulder mesh in response to an estimated biomechanical logic. The u- and v- directions (**Figure 8a**) are applied to each face of the shoulder mesh (**Figure 8b**). The complexity of the host in contrast to an idealized tube mesh representing the fish body requires the emergence of more specialized units than the ones present in the *P. senegalus*. The locations of these specialized units that have emerged through the implementation of our *MetaMesh* model to the complex mesh of human body in contrast to a tube mesh representing the fish body are identified in **Figure 8b,c**.

3.2.3 Global

The global level of organization applies optimization strategies to the hosting mesh and subsequently automates the adaptation of regional connectivity patterns and local unit shapes. To integrate functional differentiation that exists in the biological system, we assign a FC map to the mesh data structure to modulate the unit geometry of

every mesh vertex toward a protective variation of heavily articulated features (blue, FC=0) or more flexible with reduced features (red, FC=1). In combination with the neighborhood relationships, this strategy allows functional gradation across the mesh. **Figure 9a** shows how the range of values of FC is translated into a sequence of scale shapes over a torus ranging from most pronounced to least pronounced relative feature size. The most protective shape variant from the head region in the fish (c11s10) and the most flexible one from the tail region (c31s10) are mapped and morphed on the torus based on the functional gradient of FC. **Figure 9b** illustrates the mapping of the FC gradient into the human shoulder mesh with lowest values of FC in the upper arm area and highest values in the underarm. This step demonstrates a generative framework for computationally mapping segmented unit geometries to a complex surface while future iterations of the model will implement physiological data for human joints.

A global mesh optimization strategy is then applied as illustrated in **Figure 10**. The Tangential Laplacian Smoothing algorithm regularizes the hosting mesh geometry by iteratively repositioning the mesh vertices according to the geometries dictated by the FC without distorting the overall shape of the mesh. A homogenization optimization algorithm was applied to the hosting mesh. The rational behind optimizing for homogeneity is to avoid local spatial heterogeneities and discontinuous changes in the composite structure that would result in stress concentrations, weakened areas and might lead to buckling or kinking, and discomfort by the wearer. This algorithm maximizes the homogeneity across all of the quads in the mesh by replacing each vertex coordinate with a weighted average of itself and its first order neighbors [24]. In our model, a vertex displacement vector Δx_i was calculated for each vertex x_i:

$$\Delta x_i = \frac{1}{n}_i \sum_{j \in v_i} x_j - x_i$$

Vertex displacements were then applied to the vertex coordinates, $x_i' = x_i + \lambda \Delta x_i$, where λ is a fixed-scale parameter in the range $0 < \lambda < 1$. Finally, we replace the original vertex coordinates X with the new vertex coordinates X' [22]. These three steps are repeated until maximum quad homogeneity for minimum unit distortion is achieved. Here, it is important to preserve the shape of the mesh as new vertex positions are applied; we avoid mesh shrinkage by limiting vertex translation as only tangential to the mesh surface. **Figure 10** demonstrates the iterative steps for regularizing the host mesh Tangential Laplacian Smoothing through 50 iterations, while the quality of the quad ranges from distorted (red) to regular (blue). Future modification to this optimization algorithm seek to fit vertex relocation to physiological data for joint flexure, assign internal porosity to minimize weight, or distribute multiple materials for tunable composite structures with desired mechanical properties.

3.2.4 Translation to Human Mesh

We validate the *MetaMesh* computational modeling process by using it to populate a host mesh of a human shoulder with protective scales. **Figure 11** presents an overview of this process. A regular polygonal mesh of quads with boundaries was optimized from a distorted base mesh of a human shoulder. A regional directionality pattern was applied over the mesh edges to inform the construction of scale connectivity. The functional gradient was then determined according to an estimate of human biomechanics and applied to the mesh vertices. Finally, the units were adapted to the smoothed geometry through integration of neighborhood parameters encoded into the mesh vertices for each scale. The association of the local unit parameters to its neighbors in addition to the underlying mesh information (FC and regional directionality) allows for the computational translation of the segmented assembly of units adapted to the host geometry while preserving articulating connections between the units. The current composite exoskeleton design is "materials-generic" and allows for the fabrication of varied exoskeletons composed of arbitrary choice of structural materials. The weight of the exoskeleton is driven by the material choice for the rigid individual armor units and related to the composite volume fraction (volume of rigid armor units Va/volume of organic, Vo). We have calculated the volume fraction at various locations of the exoskeleton in our model and found them to be in the 1.5-1.7 range.

4. DISCUSSION

The *MetaMesh* model is a generative computational design framework for translating design principles observed in the flexible fish exoskeleton of *P. senegalus* into functionally graded structures adapted to a new host surface, e.g. a human shoulder. **Figure 11** summarizes the main steps in translational process from analysis of the biological armor into generative computation through local shape construction, regional connectivity pattern, and

global optimization and adaptation to overall geometry. *MetaMesh* attempts to solve many challenges heretofore unaddressed in architectural geometric design and flexible protective structures by developing bioinspired functional designs with components operating at multiple length scales.

Parametric Component Population (PCP) is a common method to adapt discrete geometrical components to large-scale complex shapes [26]. The host surface is normally structured as a polygonal mesh of quadrilateral faces or as a NURBS surface subdivided into u,v directions. The component's geometry is described through a parametric model and then repetitively embedded as discretized shapes on the host surface in two steps: component enclosure in an axis-aligned bounding box, and translation of the bottom-face vertex to every vertex of the mesh face in order to parametrically fill the space of the host mesh. Despite its fast distribution of volumetric units over 3D surfaces, PCP restricts the footprint of the volumetric component to the boundaries of the host quadrilaterals, which does not support certain surface contacts or tangent connections of neighboring geometries. Hence, connectivity between component features along the surface is not assured. In the *P. senegalus* exoskeleton, the peg and socket joint and overlap joint articulations are key connectivity features of the system that must be preserved when translating to a new host environment. *MetaMesh* solves this challenge by including neighborhood relationships between the units, which PCP fails to do.

Other architectural geometry strategies use quadrilateral meshes with planar faces (PQ meshes) as a rationalization strategy to build envelopes designed as discrete freeform structures [17, 27]. PQ meshes use a heuristic device to segment the envelope into flat panels for efficient fabrication. Introducing rationalization strategies early in the planning can dramatically reduce cost and risk associated with using unconventional geometry for fabrication and assembly phases [27]. The method results in the approximation of a smooth surface to a discrete one with architectural-size panels ranging from half to several meters. We chose quadrilateral polygonal meshes over triangular ones, but we did not choose to work with flat faces, to minimize the number of different components, or to maximize component size. Instead, we utilize face curvature of the mesh quad to inform the fittest unit geometry while encouraging maximum shape variation with high resolution of mesh subdivision, all to ensure adaptation and functional gradation over the host environment.

The originality of *MetaMesh* lies in its efficient framework linking experimental analytical methods (µCT and morphometric analysis) with advanced computational geometry techniques (custom data structures for polygon mesh processing and component adaptation). The results propose a novel strategy for the multifunctional adaptation of highly elaborate components to complex surfaces with tailored directionality, emergence of new unit types, and the conservation of their interconnectivity patterns. Furthermore, the computational model sets the basis for future work with different exoskeleton systems and for the optimization of requirements beyond the topology of the hosting surface, such as kinematic ranges of motion, porosity for breathability requirements, or material distribution within units to modulate materials and mechanical properties in various regions.

This proof-of-concept model uses rigid, articulated armor units with compliant substrate and interconnections to produce a flexible protective system that provides uniform coverage while preserving user mobility. Current ballistic armor technologies include Kevlar® fibers [28] and ceramic plates [29], which are not flexible enough to cover mobile joints. Alternative flexible armor systems include woven fabrics [29], mosaic tilings [30], and overlapping discs [31], which have shortcomings that diminish ballistic resistance due to inter-yarn friction or designs that inherently include vulnerable regions of armor at interfaces and areas of variable thickness. The MetaMesh model seeks to overcome shortcomings in existing armor solutions by drawing inspiration from the complex architecture of the *P. senegalus* exoskeleton, which uses a unique geometry of individual armor units combined with inter-unit articulation to yield a system with spatially homogenous thickness and no exposed, vulnerable interfaces. Segmented systems, which utilize smaller protection sub-units, have the potential to reduce cost and ease of fabrication, as well as allow for use of a wider range of constituent materials and selective replacement of damaged units. While high performance properties with strict tolerances are required for functional penetration resistance, there is great opportunity for developing novel approaches to protective joint designs where tunability is key.

In our ongoing research we are building continuity between computational construction and additive fabrication. In previous work on this research project, members of our group have successfully fabricated macroscale assemblies on flat and curved surfaces using multi-material 3D printing [14-16], as well as using materials with graded

material properties within the scale units [16]. The *MetaMesh* model preserves the closed mesh articulation and the relation amongst the units, but does not yet accommodate material articulation strategies such as layered microstructures, graded material interfaces, and internal porosity. Yet, *MetaMesh's* hierarchical organization provides the platform for additional *meta* organization principles at the local, regional, and global levels of the design process. Additionally, the specialized units for seam lines and the preservation principle of valid connection between units in *MetaMesh* allow further research and tunability of the system to the complex schema of human kinematics. Further computational development will also require focus on irregular mesh handling and other polygonal topologies to accommodate a variety of host surfaces.

MetaMesh model can be used to incorporate real physiological data and kinetic schema from the human body. This paper presents the computational design platform constructed on the logic of a biological system rather than provide for a specific bio-inspired design solution. In future the hierarchical structure of MetaMesh enables it to incorporate other concepts relevant to human physiology, such as the Lines of Non-Extension (LNE). Lines of Non-Extension, a concept first proposed by Iberall [32] and later developed and implemented in the design of "second-skin" Bio-Suit pressure garment [33], are the directions on human body that are subjected to minimal skin strain during movement. In *P. senegalus* armor, the restricted and free ranges of motion around the u- and v- directions can be analyzed akin to LNE, and could further serve as a basis for application to new kinematic constraints of human physiology [34]. For instance, *MetaMesh* could place the u-direction of a regional armor assembly on the mesh edges along the LNE of the human shoulder, while placing the v-direction along lines of maximal movement.

5. CONCLUSION

Customized computational models like *MetaMesh* provide a novel and effective method for translating the intricate, multifunctional design principles found in natural structures such as mineralized exoskeletons to synthetic, bioinspired structures. These models challenge traditional design techniques and set the basis for the incorporation of multiple layers of information, such as physiological and kinetic dimensions, at any level of the hierarchical computational data structure. *MetaMesh* is a computational model that embeds the geometric complexity of mineralized exoskeletons to enable functional gradation to the new bearer. The customized data structure provides adaptation of the system, while varying the unit features with neighborhood connectivity ensures graded overlap and interlock. With the *MetaMesh* model it is now possible to encode hierarchical relationships at local, regional, and global levels to maintain complex connectivity and functional differentiation of articulated structures on complex hosting surfaces.

Through *MetaMesh*, we see that interdisciplinary research (here drawing on experimental biology, materials science and engineering, mechanical engineering, and architecture) contributes to a better understanding of biological design principles and enhanced translation to bio-inspired and biomimetic devices. Scientific perspectives on the geometric and materials analysis in the *P. senegalus* exoskeleton better inform the designer in devising computational methods to translate designs to a new hosting surface and fabricate a functional bio-inspired system.
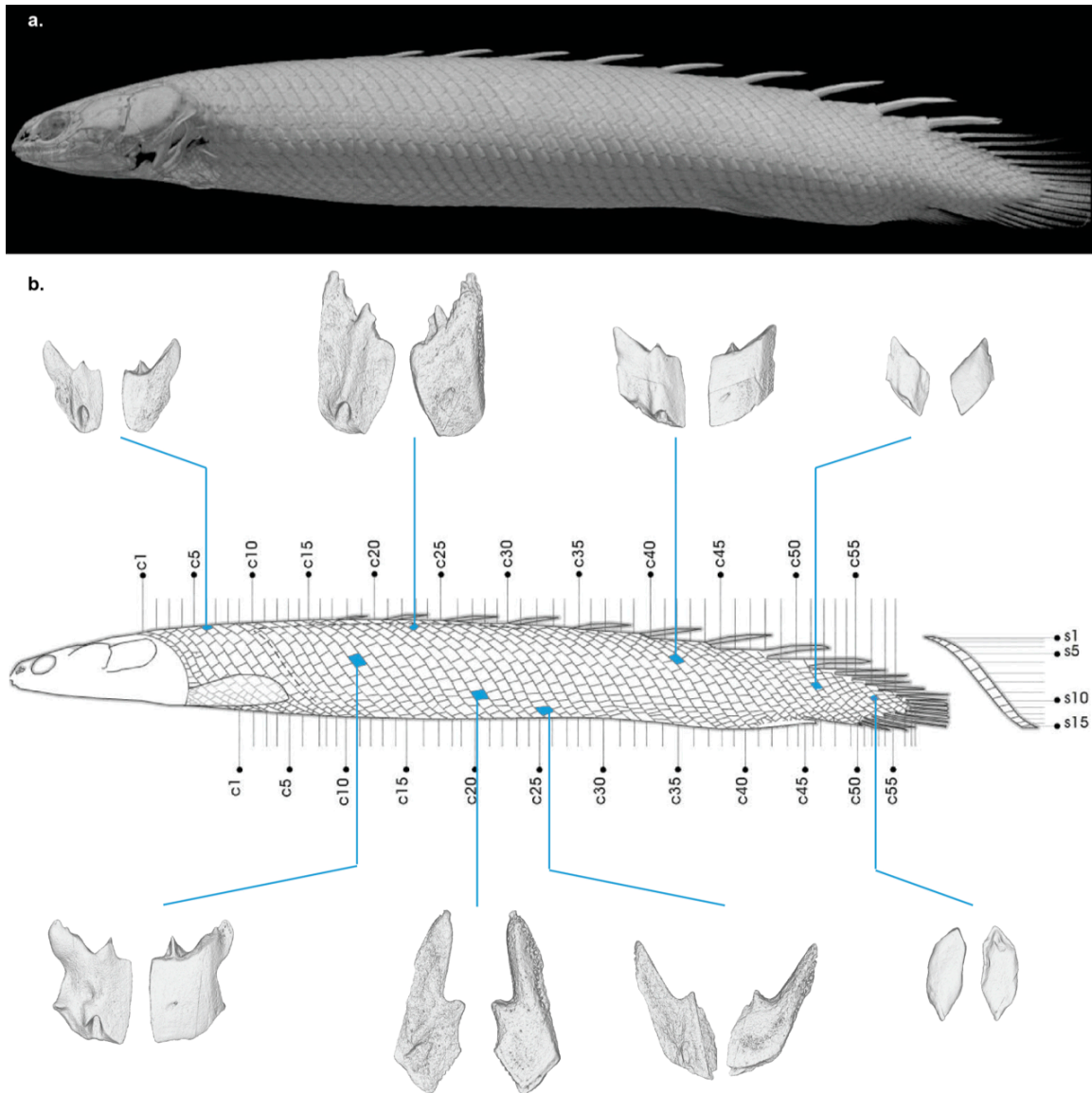
Figure 1: a. Mineralized exoskeleton of *Polypterus senegalus* (image used with permission from www.digimorph.org). **b.** Reconstructed μCT images of individual scales from different locations in the exoskeleton.

parameter	definition	calculation
PSL	peg-scale relative length	1 / 2
SR	shape aspect ratio	2 / 3
E	bounding box size	X * Y
IO	interserial overlap (v)	4 / 3
PO	paraserial overlap (u)	5 / 2
ANG	relative edge degrees	A
APL	anterior process length	6 / 7
VOL	volume (mm³)	

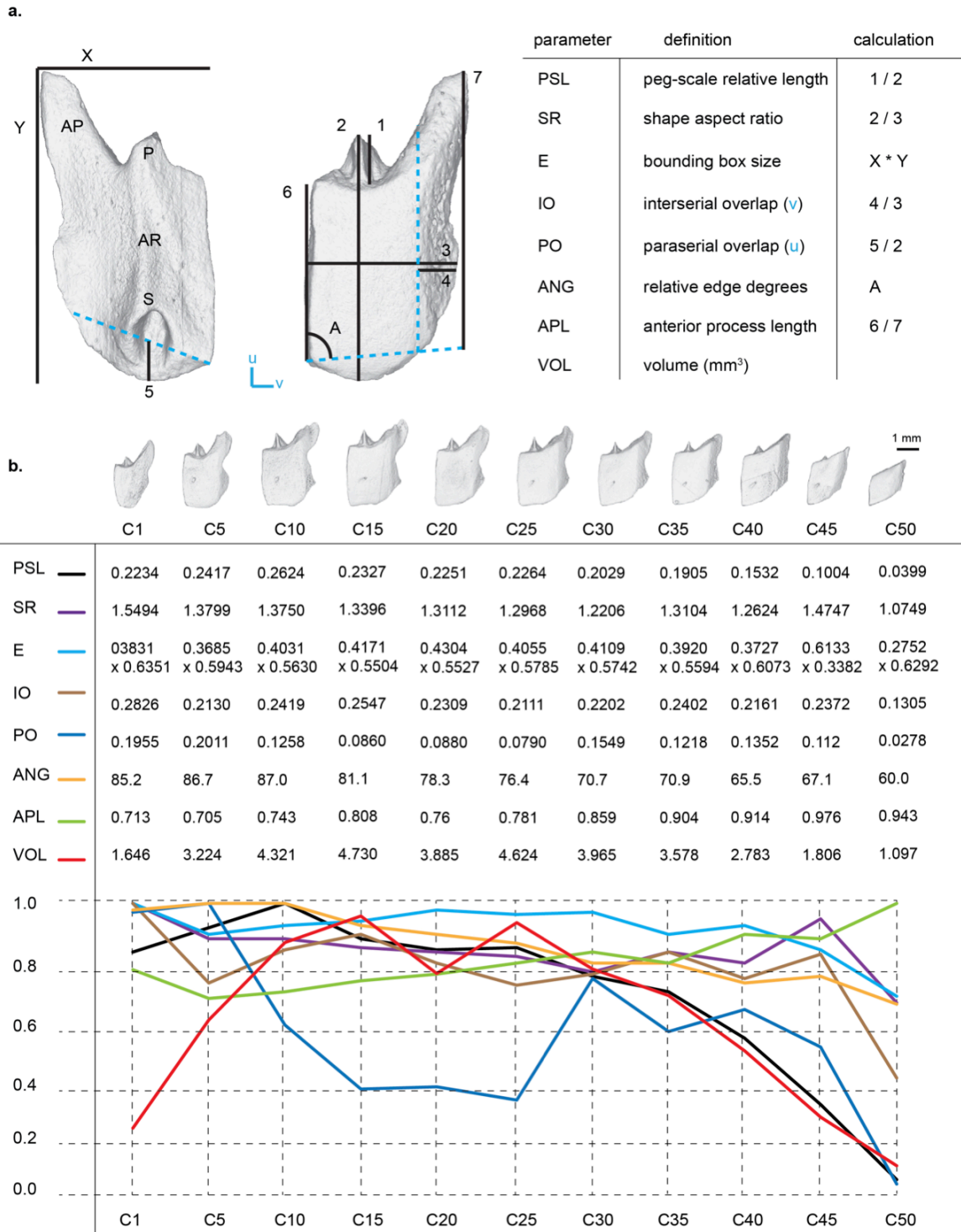|	C1	C5	C10	C15	C20	C25	C30	C35	C40	C45	C50
PSL	0.2234	0.2417	0.2624	0.2327	0.2251	0.2264	0.2029	0.1905	0.1532	0.1004	0.0399
SR	1.5494	1.3799	1.3750	1.3396	1.3112	1.2968	1.2206	1.3104	1.2624	1.4747	1.0749
E	03831 x 0.6351	0.3685 x 0.5943	0.4031 x 0.5630	0.4171 x 0.5504	0.4304 x 0.5527	0.4055 x 0.5785	0.4109 x 0.5742	0.3920 x 0.5594	0.3727 x 0.6073	0.6133 x 0.3382	0.2752 x 0.6292
IO	0.2826	0.2130	0.2419	0.2547	0.2309	0.2111	0.2202	0.2402	0.2161	0.2372	0.1305
PO	0.1955	0.2011	0.1258	0.0860	0.0880	0.0790	0.1549	0.1218	0.1352	0.112	0.0278
ANG	85.2	86.7	87.0	81.1	78.3	76.4	70.7	70.9	65.5	67.1	60.0
APL	0.713	0.705	0.743	0.808	0.76	0.781	0.859	0.904	0.914	0.976	0.943
VOL	1.646	3.224	4.321	4.730	3.885	4.624	3.965	3.578	2.783	1.806	1.097

Figure 2: Geometric analysis of scale shape variation along the fish in the head-to-tail direction. **a.** Key geometrical features of a typical scale: **P** – peg, **S** – socket, **AP** – anterior process, **AR** – axial ridge. **b. (top)** Table summarizing the morphometric parameters of 11 scales (C1-C50) normalized by maximum value, and **(bottom)** plot of the normalized scale parameters.
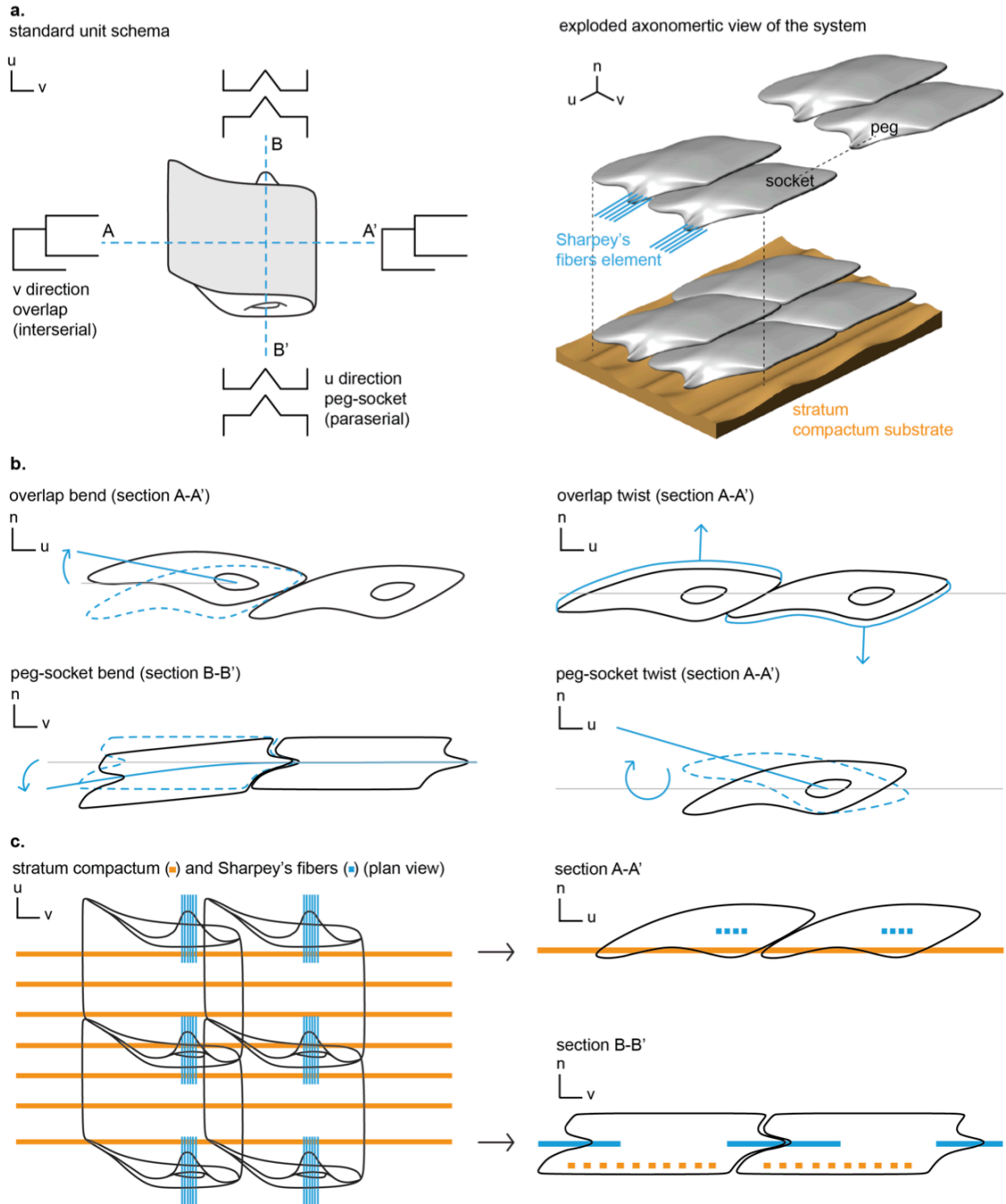
Figure 3: a. Schematic and axonometric view of unit connections within the exoskeleton assembly: u- direction peg-and-socket (paraserial) and v- direction overlap (interserial) connections, stratum compactum (orange) attaching units to the organism, and *Sharpey's fibers* (blue) attaching units to each other. **b.** Schematic of allowable ranges of motion of the unit joints: bending in overlapping joint (upper left), twisting of overlapping joint (upper right), bending in peg-and-socket joint (bottom left), twisting in peg-and-socket joint (bottom right). **c.** Schematics of the location in plan and section of the *Stratum compactum* (orange) and Sharpey's fibers (blue).
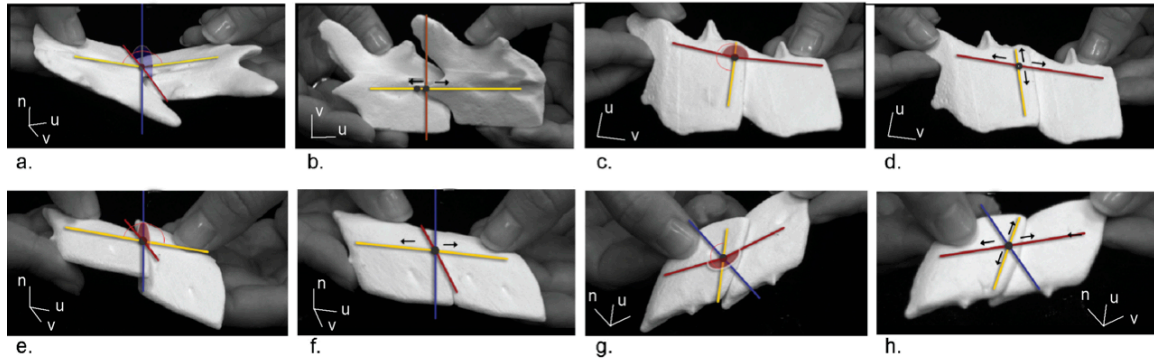
Figure 4: Allowable motions between adjacent scales in head region and tail region scale variants. Head region scales: **a.** rotation around u-axis **b.** translation along u-axis **c.** rotation around n-axis **d.** translation along v-axis. Tail region scales: **e.** rotation around u-axis **f.** translation along u-axis **g.** rotation around n-axis **h.** translation along v-axis
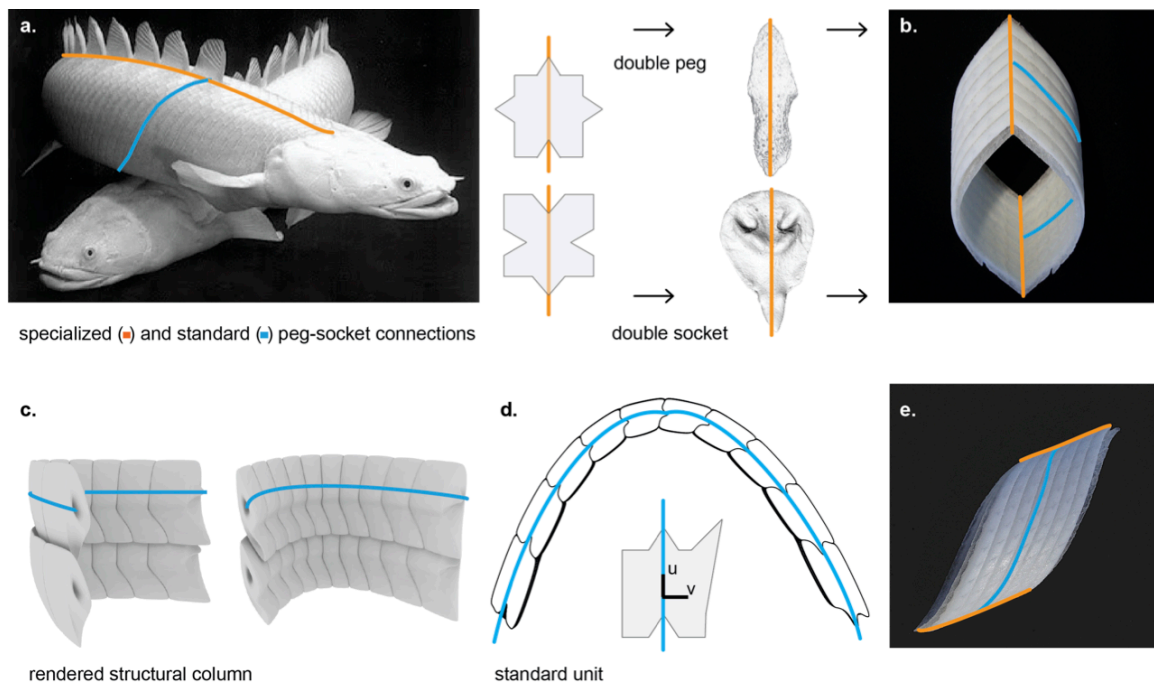

Figure 5: Lines of symmetry on the top and bottom of fish trunk. **a.** Identification of specialized(orange) and standard (blue) lines of units on the fish. **b.** 3D-printed prototype mimicking the arrayed rings in the *P. senegalus* exoskeleton and the midlines of double-peg and double-socket specialized units. **c.** 3D rendering of unit arrangement within two overlapping rings of standard units. **d.** Section through peg and socket joints showing adaptation to the curved surface. **e.** 3D-printed prototype showing the location of standard units (blue) and specialized units (orange).
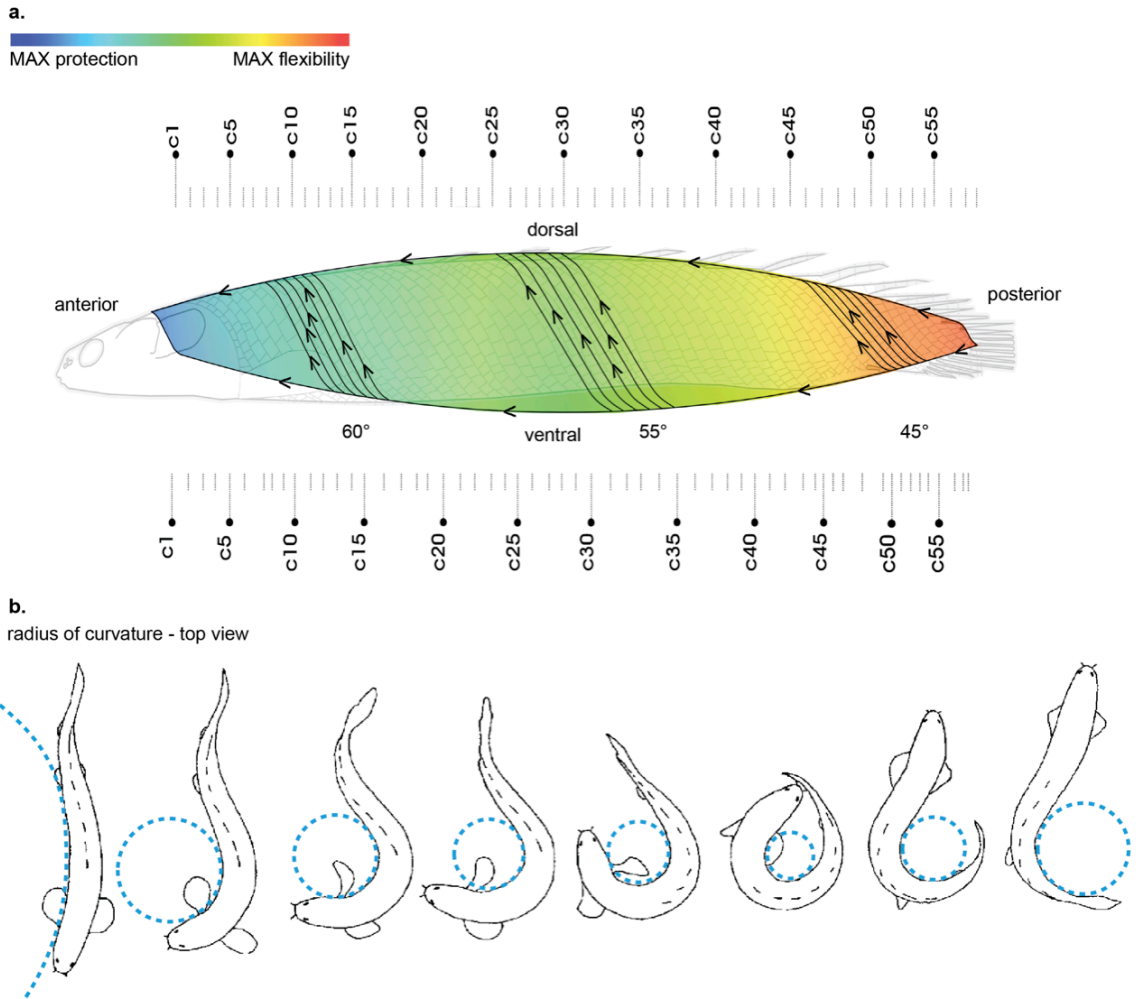
Figure 6: The global organization diagram: **a.** Spatial functional differentiation color map of unit shape ranging from maximum protection (blue) to maximum flexibility (red). **b.** Functional differentiation is adapted to the varying radii of curvature (blue dashed line) during the swimming motion of the fish (adapted from [10]).
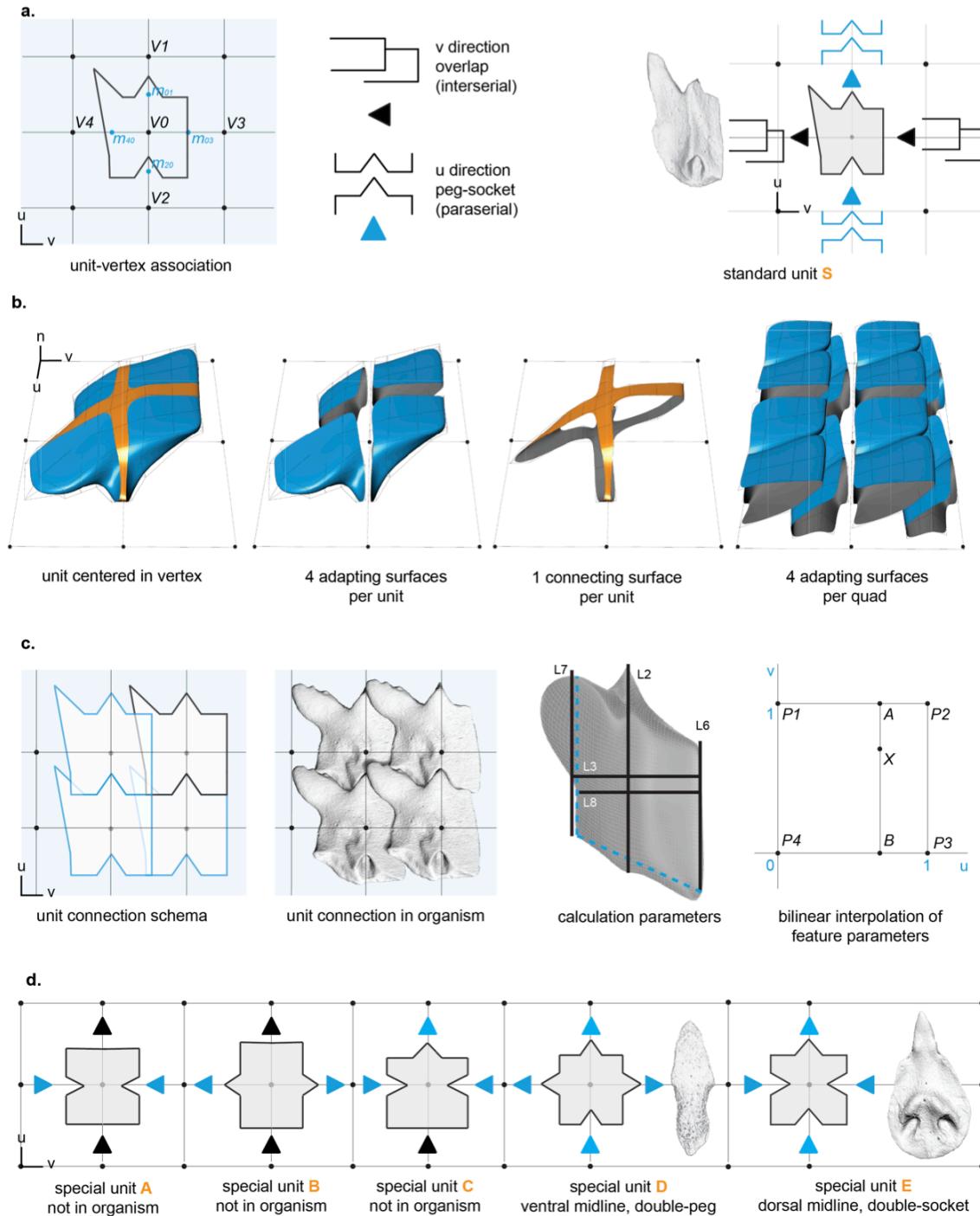
Figure 7: *MetaMesh* local unit construction. **a.** Vertex-centric (V0) unit placement on top of the underlying mesh and identification of u- (peg-socket) and v- (overlap) directions in the model. **b.** Unit construction from four connecting surfaces (blue) and a cross-shaped contact surface (orange). **c.** Arrangement of 4 standard units in the model and in the organism and calculation of the unit features from geometrical analysis parameters (L). **d.** Different specialized unit types identified by the u- and v- directions present in the organism (D, E) or defined by the directionality pattern of the new host (A, B, C).
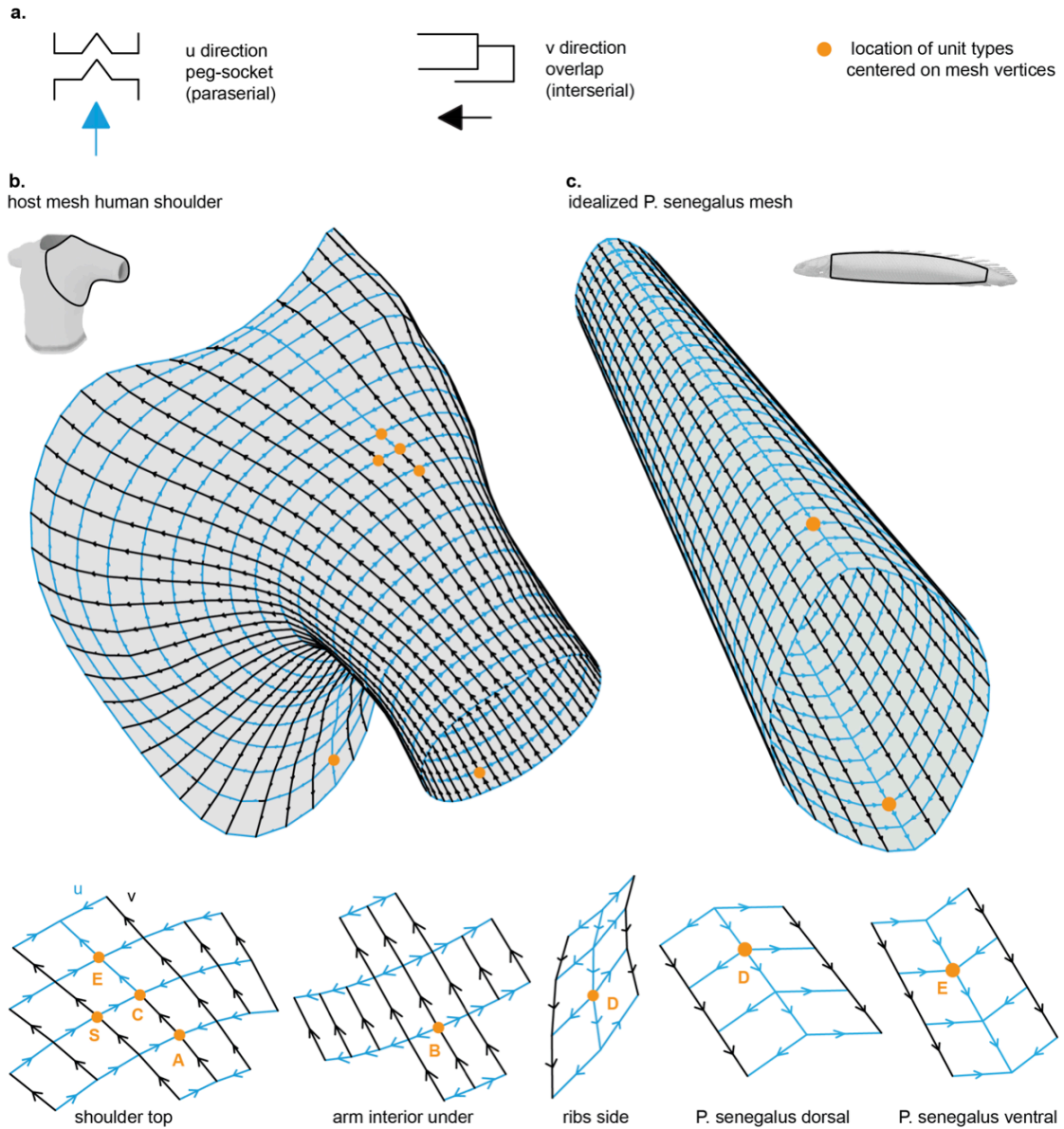
Figure 8: *MetaMesh* regional directionality pattern. **a.** Definition of peg-and-socket u- direction (blue arrows) and overlap v- direction (black arrows). **b.** Identification of directionality pattern on the human body and emergence of new specialized unit types (orange). **c.** u- and v- directions on the idealized tube-shaped body of *P. senegalus* and location of the organism's specialized units (orange).
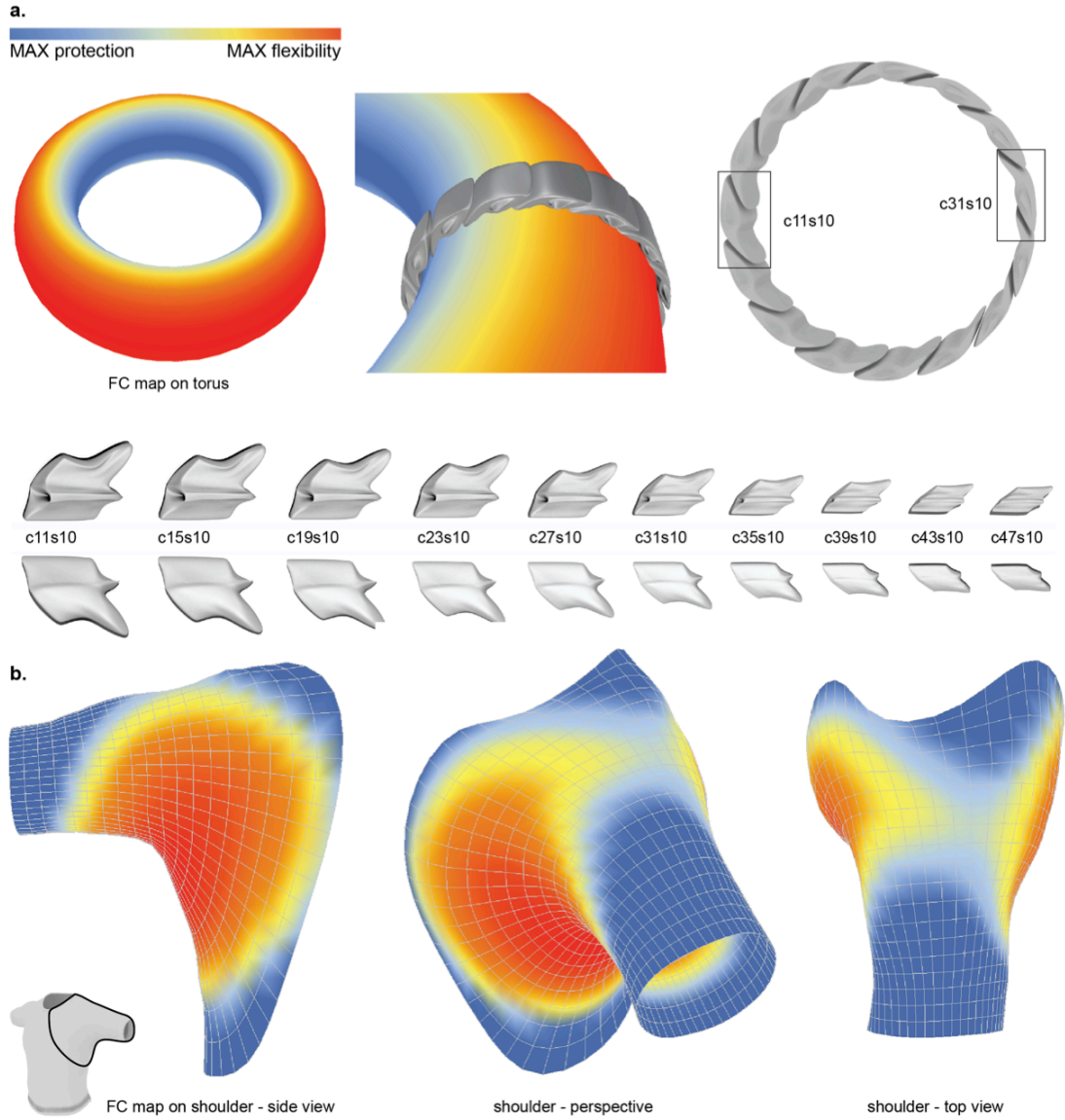
Figure 9: Variation of the unit features along an extreme band of Functional Coefficient (FC) mapping from maximum protection (blue) to maximum flexibility (red). **a.** The shape variant from head region (c11s10) and from tail region (c31s10) are mapped and morphed on the torus based on the functional gradient of FC **(bottom). b.** Identification of the estimated FC gradient on a human chest from maximum protection (blue) above the shoulder and maximum flexibility (red) in the underarm.
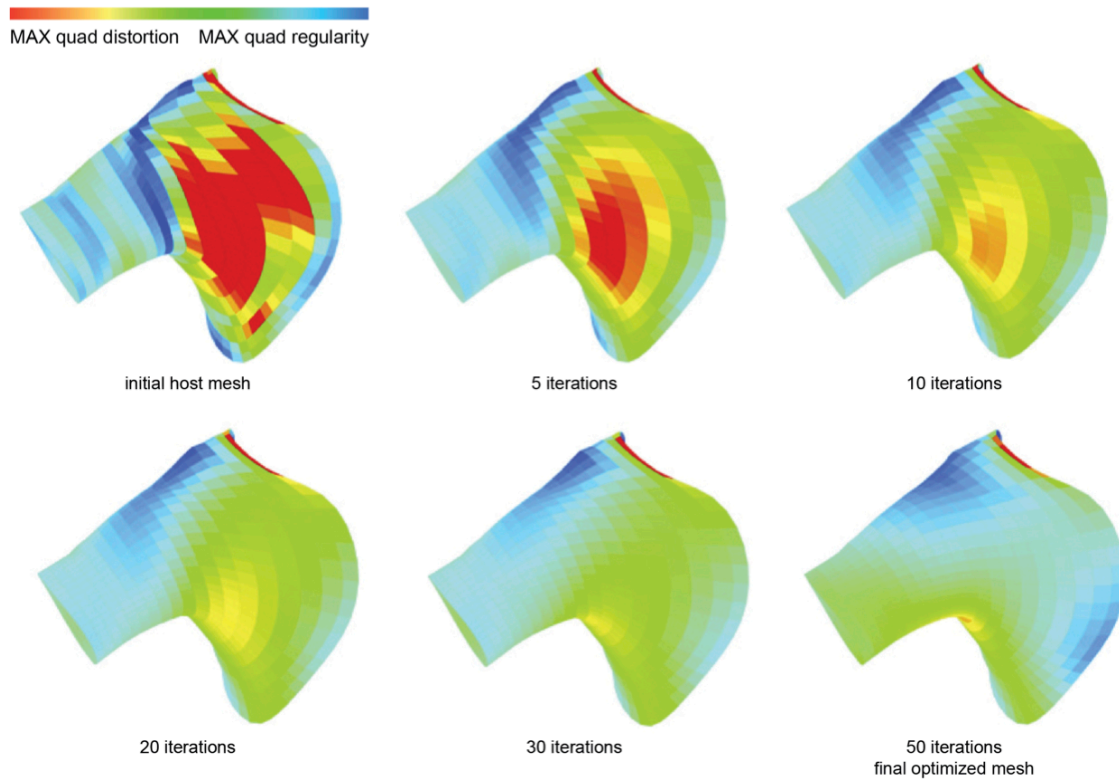
Figure 10: *MetaMesh* global iterative steps for regularizing the host mesh Tangential Laplacian Smoothing through 50 iterations. The quality of the quad ranges from distorted (red) to regular (blue).
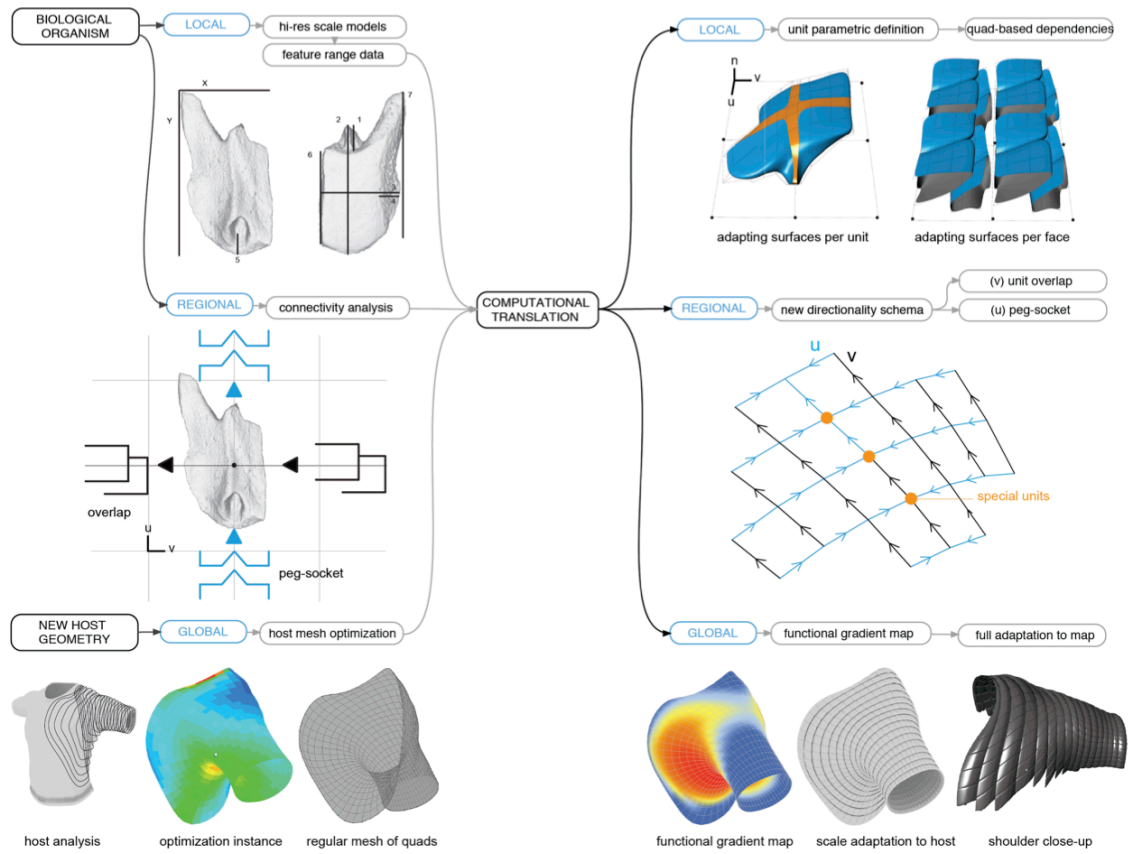
Figure 11: Graphical summary of the *MetaMesh* hierarchical computational model.

APPENDIX: ABBREVIATIONS AND SYMBOLS.

$A_{(u,v)}$	point interpolation on quad's boundary
ANG	normalized angle between two adjacent scale edges
AP	scale's front edge extension that overlaps with the scale in the next column
APL	anterior process length, the relative size of AP to scale's side length
AR	axial ridge, a protrusion on the bottom of the scale that connects the scale to the underlying organic tissue
$B_{(u,v)}$	point interpolation on quad's boundary
E	bounding box size, minimum perimeter rectangle area within which the scale can be subscribed
F	a set of polygon faces, in which a face $f = (i_1,\dots,i_{nf})$ is a sequence of non-repeating vertex indices
FC	functional coefficient, average value of the normalized geometric parameters PSL, IO, PI, and AP, indicates how developed the connective interfaces are between adjacent scales, ranging from 0 for maximum protection to 1 for maximum flexibility
IO	interserial overlap, overlap between scales in the adjacent columns
L_1	length of the peg
L_2	length of the peg and socket axis
L_3	total width of the scale
L_4	width of the overlap between scales in v- direction
L_5	width of the overlap between scales in u- direction
L_6	length of the short edge of the scale
L_7	length of the long edge of the scale
L_8	width of the scale without the overlap
LNE	Lines of Non-Extension, the directions on human body that are subjected to minimal skin strain during movement
m	a midpoint of an edge of the mesh quad
n-axis	the orthogonal direction normal to the surface of the scale
P	protruding peg, complemented with socket to form a peg-and-socket joint
P_{1-4}	points defining a mesh quad
PCP	Parametric Component Population, a common method to adapt discrete geometrical components to large-scale complex shapes
PO	paraserial overlap, an overlap between scales in the peg-and-socket joint direction
S	socket, complemented with peg to form a peg-and-socket joint
SR	shape aspect ratio, the ratio of the length of peg-and-socket axis to scale's width
u-axis	the "paraserial" direction within one column of scales, parallel to the line connecting the peg-and-socket joints
v-axis	the "interserial" direction between columns of scales, parallel to the line connecting the overlapping joints
V	vertex indices, a table of 3D vertex coordinates $X = \{x_i: I \in V\}$
PQ meshes	quadrilateral meshes with planar faces, topology of polygonal regular mesh
VOL	volume of scale in mm^3
Δx_i	vertex displacement vector, the change in mesh quad parameters due to mesh optimization
X	vertex coordinates of the mesh quad

REFERENCES

[1] M.A. Meyers, P.-Y. Chen, A.Y. Lin, Y. Seki, Biological materials: Structure and mechanical properties, Progress in Materials Science (2008) 53, p. 1-206.

[2] A.R. Studart, Towards High-Performance Bioinspired Composites, Advanced Materials, (2013) 24(37), p. 5024-5044.

[3] B. J. F. Bruet et al., Materials design principles of ancient fish armour, Nature Materials (2008) 7(9), p. 748-756.

[4] L. Ling, C. Ortiz, Pervasive nanoscale deformation twinning as a catalyst for efficient energy dissipation in a bioceramic armour**,** Nature Materials (2014), doi:10.1038/nmat3920.

[5] M.J. Connors, H. Ehrlich, M. Hog, C. Godeffroy, S.Araya, I.Kallai, D. Gazit, M. C. Boyce, C. Ortiz, Three-dimensional structure of the shell plate assembly of the chiton *Tonicella marmorea* and its biomechanical consequences, Journal of Structural Biology (2012), vol.177, pp. 314-328, http://dx.doi.org/10.1016/j.jsb.2011.12.019.

[6] D. Zhu, C. F. Ortega, R. Motamedi, L. Szewciw, F. Vernerey, F. Barthelat, Structure and Mechanical Performance of a ''Modern'' Fish Scale, Advanced Biomaterials (2011) 13, No. XX, doi: 10.1002/adem.201180057.

[7] W. Yang, I. H. Chen, B. Gludovatz, E.A. Zimmermann, R.O. Ritchie, M.A. Meyers, Natural Flexible Dermal Armor. Advanced Materials (2013), 25: 31–48, doi: 10.1002/adma.201202713.

[8] C.Ortiz, M. C. Boyce, Bioinspired structural materials, Science, 319.5866 (2008): 1053-1054.

[9] S. Gemballa, and P. Bartsch, Architecture of the integument in lower teleostomes: Functional morphology and evolutionary implications, Journal of Morphology (2002) 253(3), p. 290-309.

[10] J. Daget et al., Major discoveries on the dermal skeleton of fossil and recent polypteriforms: a review. Fish and Fisheries (2001) 2(2), p. 113-124.

[11] E.L. Brainerd, Mechanical design of polypterid fish integument for energy storage during recoil aspiration, Journal of Zoology (1994) 232, p. 7-19.

[12] J. Song, C. Ortiz, M.C. Boyce, Threat protection mechanics of an armored fish, Journal of the Mechanical Behavior of Biomedical Materials (2011) 4, p. 699-712.

[13] C. Gans, Biomechanics: An Approach to Vertebrate Biology, University of Michigan Press, 1980.

[14] S. Reichert, Reverse Engineering Nature: Design Principles for Flexible Protection Inspired by Ancient Fish Armor of Polypteridae, SMarchS thesis in Department of Architecture, MIT, 2010.

[15] K. Zolotovsky, Bio Constructs; Methods for bio-inspired and bio-fabricated design, SM thesis in Department of Architecture, MIT, 2012.

[16] S. Araya, K. Zolotovsky, Juha Song, F. Veliz, C.Ortiz, Bioinformed Performative Composite Structures: From biological micro-structures to material composites and articulated assemblies, eCAADe 31 (2013), vol.1, p.575-584.

[17] H. Pottmann, A. Asperl, M. Hofer and A. Kilian: Architectural Geometry, Bentley Institute Press (2007), ISBN 978-1-934493-04-5.

[18] R.B. Clark, J.B. Cowey, Factors controlling the change of shape of certain nemertean and turbellarian worms, J. Exp. Biol. (1958) 35, no. 4, p.731-748.

[19] M.R. Hebrank, Mechanical properties and locomotor functions of eel skin, Biol. Bull.(1980)158, pp.58-68.

[20] M. Mäntylä, An introduction to solid modeling, Computer Science Press, 1988.

[21] M. Mäntylä, Topological analysis of polygon meshes, Computer-Aided Design, 10(7):228–234, 1983.

[22] G. Taubin, Introduction to Geometric Processing through Optimization, IEEE Computer Graphics and Applications (2012) 32(4): 88-94.

[23] L. Kobbelt, M. Botsch, Freeform Shape Representations for Efficient Geometry Processing, Shape Modeling International. pp. 111–118.

[24] Y. Zhang, R. Bajaj, G. Xu, Surface smoothing and quality improvement of quadrilateral/hexahedral meshes with geometric flow, 14th International Meshing Roundtable Proceedings (2005), John Wiley & Sons, pp. 449–468.

[25] C. Yuksel, J.M. Kaldor, D. L. James, S. Marschner, Stitch Meshes for Modeling Knitted Clothing with Yarn-level Detail ACM Transactions on Graphics, Proceedings of SIGGRAPH (2012) 31, 3.

[26] I. Rajaa, Paneling Tools for Grasshopper, Rhinoceros Development team, Robert McNeel & Associates, 2013 (http://wiki.mcneel.com/labs/panelingtools).

[27] A. de Leon, Rationalization of freeform façades: a technique for uniform hexagonal paneling, Beyond codes and pixels: CAADRIA, 2012, pp 253-262.

[28] Kevlar® Aramid Fiber, DuPont http://www.dupont.com/products-and-services/fabrics-fibers-nonwovens/fibers/brands/kevlar.html.

[29] N. V. David, J. Q. Zheng and X.-L. Gao, Ballistic Resistant Body Armor: Contemporary and Prospective Materials and Related Protection Mechanisms, Applied Mechanics Review, 62(5), 050802 (2009), doi:10.1115/1.3124644

[30] ArmorFlex® articulating concrete block mats http://www.conteches.com/products/erosion-control/hard-armor/armorflex.aspx.

[31] Pinnacle Armor® DRAGON SKIN® http://www.pinnaclearmor.com/body-armor/dragon-skin.php.

[32] A.S. Iberall, The Experimental Design of a Mobile Pressure Suit, Journal of Basic Engineering (1970) pp. 251-264.

[33] A.M. Wessendorf, D.J. Newman, Dynamic Understanding of Human-Skin Movement and Strain-Field Analysis, *Biomedical Engineering, IEEE Transactions on*, vol.59, no.12, 2012, pp.3432,3438. doi: 10.1109/TBME.2012.221585

[34] K. Bethke, D.J. Newman, R. Radovitzky, Creating a skin strain field map with application to advanced locomotion spacesuit design, Proceedings of the XXth congress of the international society of biomechanics (ISB), (2005) Cleveland, OH.

VITAE

Designer Neri Oxman is the Sony Corporation Career Development Professor and Assistant Professor of Media Arts and Sciences at the MIT Media Lab. Her group Mediated Matter explores how digital design and fabrication technologies mediate between matter and environment to radically transform the design and construction of objects, buildings, and systems. Oxman was named to ICON's list of the top 20 most influential architects to shape our future (2009), and was selected as one of the 100 most creative people by FASTCOMPANY (2009). In 2008, she was named "Revolutionary Mind" by SEED Magazine. Her work has been exhibited at MoMA (NYC) and is part of the museum's permanent collection. In 2012 the Centre Georges Pompidou Museum (Paris, France) acquired her works for its permanent collection.

Professor Mary C. Boyce is the Ford Professor of Engineering and Department Head of Mechanical Engineering at the Massachusetts Institute of Technology. Her research areas focus primarily on the mechanics of elastomers, polymers, polymeric-based micro- and nano-composite materials, lattice-structured materials, natural materials, and biological macromolecular networks, with emphasis on identifying connections among microstructure, deformation mechanisms, and mechanical properties. She has published over 100 journal papers in the field of mechanics and materials; and has mentored 36 SM Thesis students and 20 PhD students. Professor Boyce has been the recipient of numerous awards and honors recognizing her research and teaching efforts.
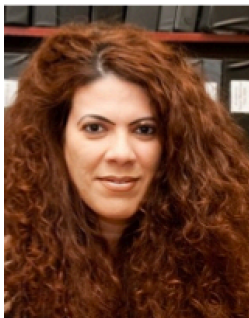
Christine Ortiz is the Dean for Graduate Education and Professor of Materials Science and Engineering at the Massachusetts Institute of Technology. Prof Ortiz's research programme focuses on the multiscale mechanics of structural biological materials (musculoskeletal and exoskeletal), with the primary goal being to quantify and understand new mechanisms, phenomena, and design principles and how they determine function, quality, and pathology. Dr. Ortiz has over 140 scientific publications in more than 20 academic journals, including Science, Nature Materials (cover), Nano Letters, Physical Review Letters, Proceedings of the National Academy of Sciences USA, Biophysical Journal, Tissue Engineering, and the Journal of Biomechanics.

Jorge Duro-Royo is a Research Assistant at the Mediated Matter Group in the Media Laboratory, Massachusetts Institute of Technology, where he focuses on Computational Design. He is an Architect by the Polytechnic University of Catalonia School of Architecture (UPC-ESTAV) and a Mechanical Engineer by the Polytechnic University of Catalonia School of Industrial and Aeronautic Engineering (UPC-ETSEIAT) where he graduated with honors. In 2010 completed a 'Master in Advanced Design and Digital Architecture' at the Pompeu Fabra University (UPF). In 2012 he started collaborating with the Ortiz Structural Biomaterials Laboratory in the Department of Materials Science and Engineering, MIT.

Katia Zolotovsky is a PhD student in the Design and Computation Group in the Department of Architecture, MIT. She also works as a Research Assistant in the Ortiz Structural Biomaterials Laboratory in the Department of Materials Science and Engineering, MIT. She holds undergraduate degrees in both biology and architecture from the Technion, Israel Institute of Technology and her research approach combines science and design methodologies. Her research interests lay in representation, translation, and application of naturally occurring material organization principles for synthetic designs. In 2013 she initiated and co-taught a graduate class "4.552 Synthetic Exoskeletons: Translation from Biological to Design System" at MIT.

Laia Mogas Soldevila is a Research Assistant at the Mediated Matter Group, MIT Media Lab, focusing on Material Systems Design. She is an Architect by the Polytechnic University of Catalonia School of Architecture (UPC-ETSAV) where she graduated with honors with a minor in Visual Arts. In 2010 completed a Master in 'Advanced Design and Digital Architecture' at the Pompeu Fabra University (UPF). In 2010-2011 started a postgraduate program in 'Architecture, Energy and Environment' in UPC-ETSAB with a Doctoral grant. She has been awarded with the LaCaixa Foundation fellowship 2011-2013 to complete her 'Master of Science in Architecture Studies at the Massachusetts Institute of Technology in the Design and Computation Group.

Swati is a PhD student at MIT in the Department of Materials Science & Engineering at MIT. She holds a BS in Materials Chemistry from Carnegie Mellon University. She also holds an MPhil in Micro- and Nanotechnology Enterprise from the University of Cambridge, which she attended as a Churchill Scholar in 2010-2011. She was awarded the NSF Graduate Research Fellowship for her doctoral research with the Ortiz Structural Biomaterials Laboratory, which focuses on the materials and mechanical design principles of armored exoskeletons and biomimetic design of flexible protection. She won the award for "Best Student Paper" on her research talk at the SICB Annual Meeting in January 2013.